CORRELATION OF LANGMUIR ISOTHERM, OPTICAL, SURFACE POTENTIAL AND MORPHOLOGICAL CHARACTERIZATIONS OF TWO FUNCTIONALIZED DIHYDROXYCALIX[4]ARENE FOR LEAD CATION ENTRAPMENT

Faridah Lisa Supian[1*], Noor Azyyati Azahari[1], Yusnita Juahir[2], Nur Farah Nadia Abd Karim[1] and Abdullah F. Naim[3]

[1]Department of Physics, Faculty of Science and Mathematics, Universiti Pendidikan Sultan Idris, 35900 Tanjong Malim, Perak, Malaysia
[2]Department of Chemistry, Faculty of Science and Mathematics, Universiti Pendidikan Sultan Idris, 35900 Tanjong Malim, Perak, Malaysia
[3]Department of Physics, College of Science, King Faisal University, Saudi Arabia

*faridah.lisa@fsmt.upsi.edu.my

Abstract. The versatilities of calixarenes have been known primarily in the host-guest world. In this work, two calix[4]arenes, namely C-DHC4 and N-DHC4, possess the same lower rim but are distinct in the upper rim. The Langmuir Isotherm and optical properties have been carried out using Langmuir–Blodgett trough and UV-Visible spectroscopy, respectively. The topographical image of the calix[4]arenes has been observed using FESEM, and lead cation entrapments of these calix[4]arenes have been inspected using the surface potential sensor. The isotherm graph revealed the size of each calixarene; C-DHC4 ~ 1.90 nm^2 and N-DHC4 ~ 2.10 nm^2. The UV-Visible result demonstrated that each calix[4]arene has two firm absorption peaks where C-DHC4 has two broad peaks, which lie in 261 and 330 nm, while N-DHC4 has two shoulders at 275 and 282 nm. FESEM images have shown the formation of calix[4]arene nanocluster. Further monitoring on the surface potential and effective dipole moment indicate that C-DHC4 perform significant and stable results in detecting Pb^{2+} cations compared to N-DHC4. This study has demonstrated that detection limit as low as 1.25 x 10^{-2} mM, making the ΔV and $\mu_{\perp}$ measurements a reliable method for detecting Pb^{2+} ions and their potential in this nanosensor field.

Keywords: Calixarenes, surface pressure, surface potential, FESEM, lead sensor

Article Info

Received 17th September 2021
Accepted 27th November 2021
Published 20th December 2021

ISSN: 1823-7010, eISSN: 2600-7444

Introduction

The remarkable feature of the calixarene host-guest molecule has been widely and rapidly recognized for its applications [1-4]. Furthermore, various functional groups can be synthesised and designed to fit as a molecular device for specific ion sensing in current research [5-7].

Calixarenes, a class of macrocyclic compounds, made up of phenol units linked by methylene bridged that provide flexibility to the molecule, are very attractive because of their ability to bind a variety of ions [8]. Amphiphilic calixarenes which are insoluble in water but soluble in an organic solvent, are "surfactants with a host-guest recognition site" [9]. A guest molecule must be stabilized, transported, or protected in aqueous media. As amphiphilic calixarenes can interact with aqueous systems, they are particularly interested in biological and environmental applications, e.g., wastewater treatment, medical diagnosis, and highly sensitive and selective sensors [10,11].

This research aims to determine the behaviour of two types of calix[4]arenes on the air-water interphase, optical characteristics and to study the interaction of both calixarenes as a host on the metal cation guest as illustrated in Figure 1.

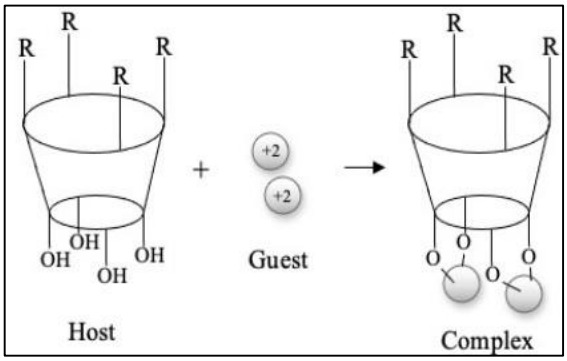

Figure 1. Host-guest interaction

Materials and Methods

Calix[4]arenes. Calix[4]arenes were obtained from the Institute of Technology, Tallaght, Dublin, Ireland, while the chloroform (>99.8% purity) and ethanol (>99.4% purity) were purchased from Fisher Scientific. The molecular structures, IUPAC name and CPK Modeling (Corey Pauling and Koltun) of both calix[4]arenes are shown in Table 1. Each calixarene was then made into a solution of a concentration of 0.20 mg/ml, a mixture of chloroform and calixarene powder.

Table 1. Molecular structure of C-DHC4 and N-DHC4

Material	IUPAC Name	Molecular structure	CPK Modeling
C-DHC4	5,11,17,23-tetra-tert-butyl-25,27-diethoxycarbonyl methyleneoxy-26,28-dihydroxycalix[4]arene	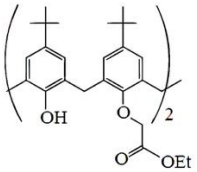	
N-DHC4	5,17,dinitro-11,23-ditert-butyl-25,27-diethoxycarbony lmethyleneoxy-26,28-dihydroxycalix[4]arene	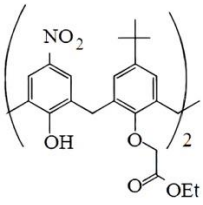	

The Π–A isotherms. Surface pressure–area (Π–A) isotherms were measured on a KSV 2000 Langmuir–Blodgett system (KSV Instruments Ltd., Finland) with deionized water as subphase. The water was purified with a Millipore Milli-Q system with a resistivity of 18.2 MΩ. The calix[4]arene solution was spread carefully using a microsyringe onto water subphase with varying volumes. After 10 minutes, the monolayer film was compressed at a 12 mm/min speed with a measurement accuracy of 0.1 mN/m. The Π–A isotherms were measured several times to ensure the measurements were reproducible. All experiments were performed at a room temperature of 23°C and kept constant within ±2°C. From the isotherms graph, extrapolation on the mean molecular surface area (A_{lim}) and comparing with the CPK modelling, the conformation and orientation of the calixarenes on air/water interphase can be predicted [11].

Optical properties of calix[4]arenes. Ultraviolet-Visible absorption spectra of both calixarenes solutions were recorded on a JASCO V-570 UV/VIS spectrophotometer [12] and using the quartz cuvettes.

Field Emission Scanning Electron Microscope with Energy Dispersive X-ray Analysis. This work used a high-resolution Field Emission Scanning Electron Microscope (FESEM) with Energy Dispersive X-ray (EDX) model Hitachi SU 8020 UHR. This enables to visualisation of the morphology and identifying the elements of the sample [13]. The accelerating voltage (V_{acc}) was set to 3 kV, the working distance was set to 5 mm and a magnification of 10.0 k to 50.0 k.

Surface potential and Effective dipole moment measurements: Capability of Calix[4]arene in Lead (Pb^{2+}) cation entrapment. The capability of calix[4]arene in Pb^{2+} cation entrapment may be measured by investigation of the maximum surface potential (ΔV_{max}) and maximum effective dipole moment ($\mu_{\perp max}$) of these calix[4]arenes within Pb^{2+} Solution. The ΔV measurements are used as a supplementary source of information on the arrangement of molecules on the water surface [11]. The ΔV was measured by

KSV Surface Potential Sensor (S-POT) as shown in Figure 2 with a vibrating plate condenser connected to the counter electrode placed at the bottom of the trough. The vibrating plate is placed approximately 1.00 -2.00 mm from the water surface, and the sensitivity of the device is ± 1.00 mV. The ΔV was simultaneously recorded with Π-A isotherm reading.

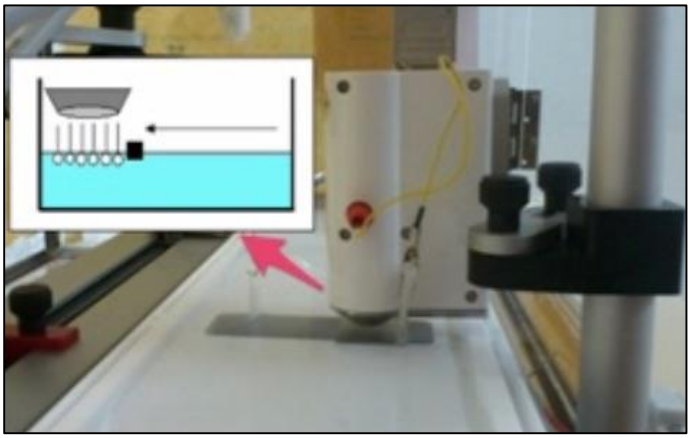

Figure 2. KSV Surface Potential Sensor (SPOT)

Effective dipole moment, $\mu_{\perp}$ is the vertical component of dipole moment in the monolayer [14]. The maximum value of ΔV can be obtained by measuring the maximum value of $\mu_{\perp}$ at the same area per molecule from the ΔV-A and $\mu_{\perp}$-A isotherms [15]. The ΔV and $\mu_{\perp}$ are related by the Helmholtz equation in (1).

$$\Delta V = \frac{\mu_{\perp}}{\varepsilon_o \varepsilon A} \quad (1)$$

where ΔV is the measured surface potential, $\mu_{\perp}$ is average μ normal to the monolayer plane, ε_o is the vacuum permittivity, and A is the mean molecular area of the monolayer.

Results and Discussion

Surface pressure-area (Π-A) isotherms. The Π-A isotherms of C-DHC4 and N-DHC43 are shown in Figure 3. Using a microsyringe, 100 µl of each material was spread to form a Langmuir film on the air-water interface. The similarity of these two calix [4]arenes is the lower rims but different upper rims. Therefore, the estimated mean molecular surface area (A_{lim}) of C-DHC4 and N-DHC4 is within the close range of ~ 2.00 nm^2.

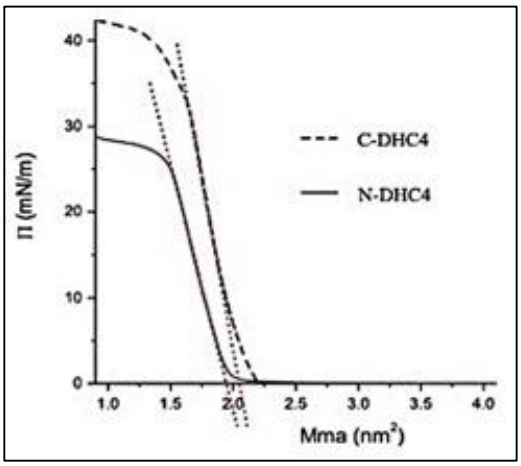

Figure 3. Comparison of Π-A isotherm of C-DHC4 and N-DHC4 at 100 µl spreading volume

Initially, the surface pressure was nearly zero, then increased linearly, after which it increased sharply at the lower mean molecular area before collapsing. When the barrier is slowly closed, the molecules begin to move nearer to each other from the gaseous phase, liquid phase, and solid phase, resulting in the Π-A curve shifting towards the left. Finally, it reached ~ 28.0 mN/m for spreading volume of 100 µl for N-DHC4. At higher pressure, the monolayer was of poor quality. The monolayer was very rigid, collapsing rapidly, and appearance of irregular [16]. From the isotherms, the A_{lim} occupied by each N-DHC4 molecule was estimated by extrapolating the linear portion of each curve to a surface pressure equal to zero (Red dotted line in Figure 3). Such extrapolations are routinely used to estimate the surface area per molecule in films that are condensed. These extrapolations yielded A_{lim} resulting in a similar orientation as C-DHC4.

The effect of increased loading of N-DHC4 was studied as shown in the isotherms graph. By calculating and comparing the theoretical cross-sectional area value from CPK modelling [17], both calix[4]arenes possess a parallel (∥) orientation of the plane of the calixarene ring with respect to the plane of the water surface, as shown in Figure 4. From the CPK value, the cross-sectional value is 2.00 nm^2. Compared with CPK modelling, which had been a powerful method in estimating the orientation of molecules at the air/ water surface, these measurements yield a parallel orientation of the plane of the calixarene ring and water plane [18].

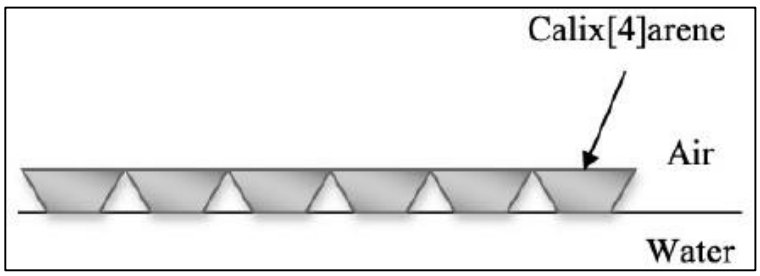

Figure 4. An illustration of calix[4]arene parallel orientation on water

Optical properties of calix[4]arenes. Figure 5(a) shows the UV-visible spectra of C-DHC4 in chloroform. It can be observed that the absorption spectrum has two broad peaks, which lie in 261 and 330 nm, respectively. The two peaks are due to the absorption band of the benzene ring corresponding to the excitation of a π electron of the conjugated system to a π* orbital. Thus, when the concentrations of C-DHC4 are increased, the absorption peak rises as well.

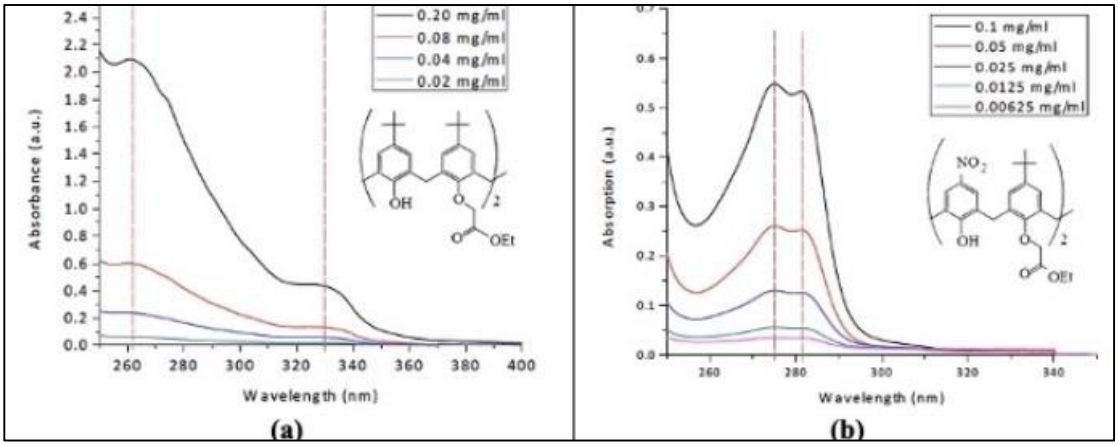

Figure 5. UV-Visible spectra of (a) C-DHC4 and (b) N-DHC4

The UV–Visible spectra of the N-DHC4 are shown in Figure 5(b). These samples have strong absorption bands in the range of 260–300 nm. N-DHC4 has two shoulders that resemble strong absorption peaks at 275 and 282 nm. All the strong absorptions are assigned to π-π* and n-π* transition due to chromophores at the upper rim of N-DHC4.

FESEM Analysis. Figure 6(a) and (b) shows the top view of the FESEM image of C-DHC4 and N-DHC4, respectively, at 50.0 k magnifications for the LB films. Certainly the clusters could be seen formed in both calix[4]arenes LB films. For C-DHC4 in Figure 6(a), the particles were neatly assembled and practically display similar sizes. The sizes of the N-DHC4 are exposed in Figure 6(b) where the sizes of the particles are irregular. Prominently, spacing between the particles are noticeably emerging which implied that the isotherm preasure was inadequate while performing the LB films process. These leads to the theoretically relation to the analogy; phase of the films is interpreted as the C-DHC4 revealing the solid phase while N-DHC4 is in the gas-liquid phase. Both depict almost spherical particles of calix[4]arene, which confirm the theory of vase-like and CPK model exactly [4,9,18].

Figure 6(c) gives the EDX distribution of elements for the deposited N-DHC4 Langmuir-Blodgett films. EDX analyses of these particles in FESEM micrographs at various locations has shown that it consists of carbon (C), nitrogen (N) and oxygen (O) in the composition of the prepared film, which substantiated with the molecular components.

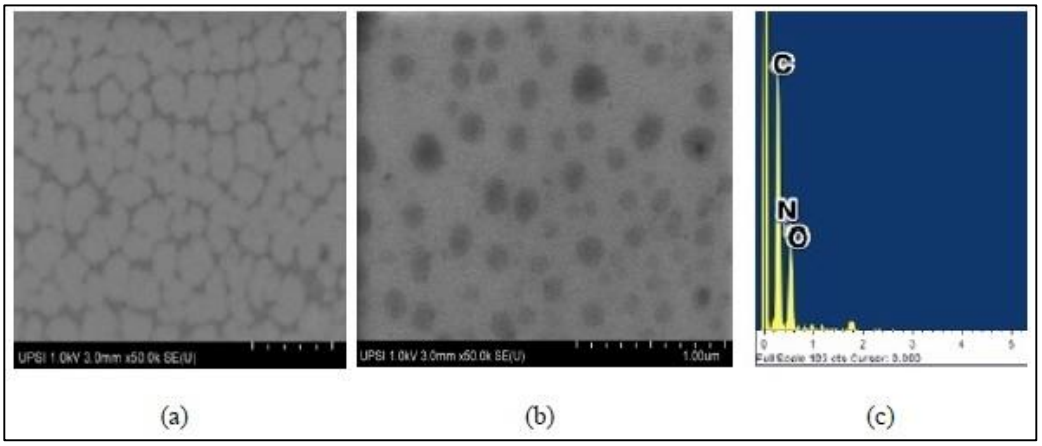

Figure 6. FESEM images of N-DHC4 LB films at 50.0 k magnification of (a) C-DHC4 and (b) N-DHC4 and (c) EDX element distribution of LB film

Surface potential and Effective dipole moment measurements: Capability of C-DHC4 and N-DHC4 in Lead cation entrapment. Figure 7 shows the overall ΔV_{max} and $\mu_{\perp max}$ characteristics of C-DHC4 in the full range of Pb^{2+} ion concentrations. Based on Figure 7(a), ΔV_{max} gradually rises to ~ 530 mV and become constant for concentrations of 2.50 x 10^{-2} mM. This suggested that the potential rises consistently as an increasing number of Pb^{2+} ions are incorporated into the C-DHC4 monolayer, but once the maximum number of ions have been achieved, no further increase in ΔV_{max} is possible. The results are complemented with the calculated value of $\mu_{\perp max}$ where the ions begin to interact with C-DHC4 until equilibrium is achieved. At concentration ~3.00 x 10^{-2} mM, the $\mu_{\perp max}$ is ~2.70 D and started to stable. While the ΔV_{max} recorded was 552 mV. This indicates that the most significant number of ions bind with C-DHC4 has been reached. Hence, ion sensing of Pb^{2+} ions using C-DHC4 can be achieved with the highest detection limit of 5.00 x 10^{-2} mM.

The ΔV_{max} and $\mu_{\perp max}$ data of N-DHC4 are plotted in Figures 7(c) and 7(d) as a function of concentration, respectively. In Figure 7(c), the ΔV_{max} increases slowly before the value slightly decrease and is stable for 5.00 x 10^{-2} mM concentration. However, when the concentration of Pb^{2+} is raised, the potential increase until it reaches the highest value. This is due to the optimum number of Pb^{2+} has been trapped at the lower rim of N-DHC4. Hence, the optimized value of $\mu_{\perp max}$ of N-DHC4 incorporating Pb^{2+} is ~1.80 D at 6.25 x 10^{-2} mM, and ΔV_{max} is 376 mV. Table 2 represents the summary data of A_{lim}, ΔV_{max} and $\mu_{\perp max}$ of C-DHC4 and N-DHC4 in Pb^{2+} solution. From the data, a detection is as low as 1.25 x 10^{-2} mM and therefore manifest promising potential for Pb^{2+} ions detection for C-DHC4 and N-DHC4.

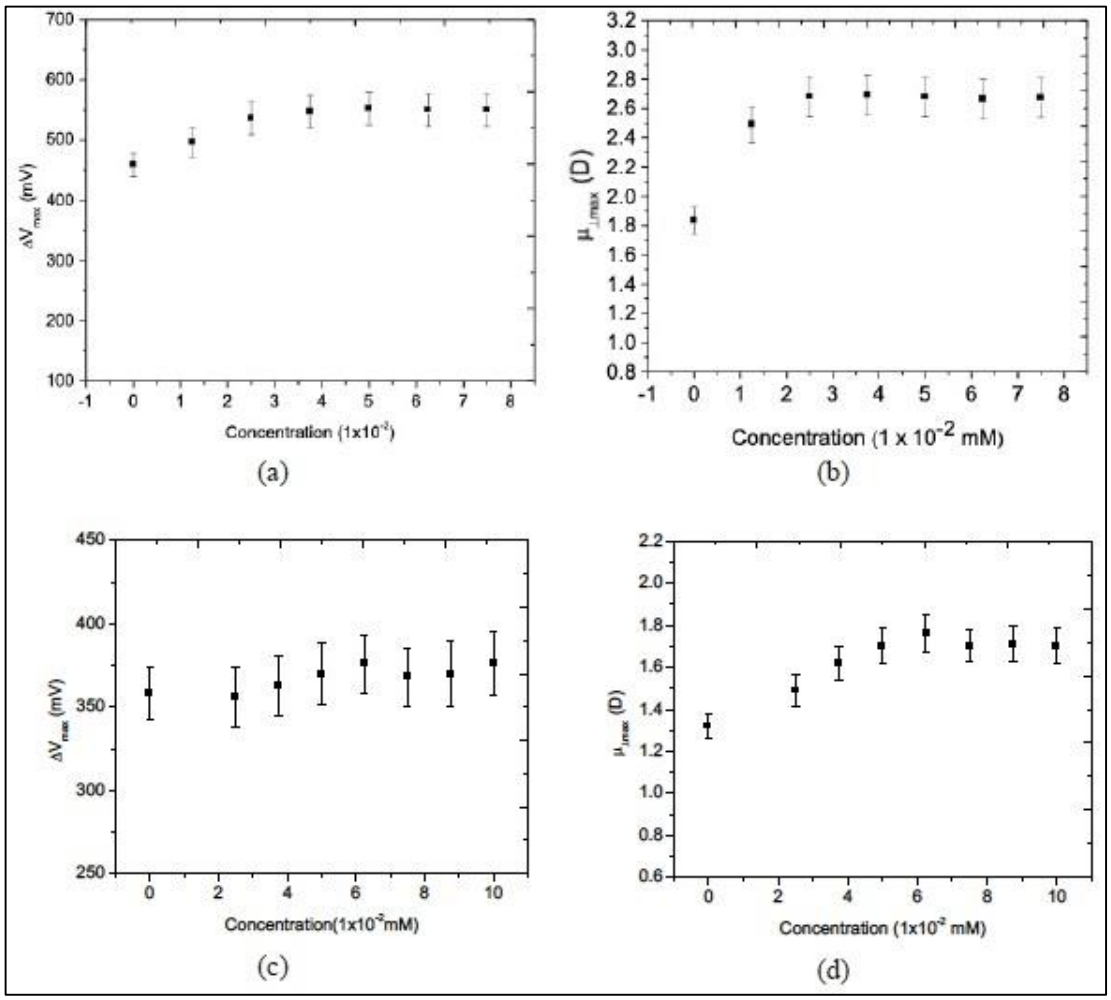

Figure 7. C-DHC4 with increasing concentration of Pb^{2+} ion of (a) ΔV_{max} (b) $\mu_{\perp max}$, and N-DHC4 with increasing concentration of Pb^{2+} ion (c) ΔV_{max} and (d) $\mu_{\perp max}$

Table 2. Summary of A_0, ΔV_{max} and $\mu_{\perp max}$ of C-DHC4 and N-DHC4 in Pb^{2+} solution

Subphase	Concentration ($1x10^{-2}$ mM)	C-DHC4			N-DHC4		
		A_0 (nm^2)	ΔV_{max} (mV)	$\mu_{\perp max}$ (D)	A_0 (nm^2)	ΔV_{max} (mV)	$\mu_{\perp max}$ (D)
Water	0	1.68	460	1.80	1.55	359	1.30
Pb^{2+}	1.25	2.09	496	2.40	-	-	-
Pb^{2+}	2.50	2.04	536	2.60	1.70	356	1.40
Pb^{2+}	3.75	2.03	547	2.60	1.78	363	1.60
Pb^{2+}	5.00	1.84	552	2.60	1.60	370	1.70
Pb^{2+}	6.25	1.91	530	2.60	1.71	376	1.70
Pb^{2+}	7.50	2.00	502	2.60	1.70	368	1.70
Pb^{2+}	8.75	-	-	-	1.72	370	1.70
Pb^{2+}	10.00	-	-	-	1.71	376	1.70

Conclusion

This work has investigated two types of Calix[4]arenes that possess the same lower rim but are divergent in the upper rim. Molecular orientations and studies have been carefully examined at the optimum condition. By extrapolation of the isotherm, the size of each calix[4]arene has been deduced, which is ~ 1.90 to 2.10 nm^2 . UV-Visible results explain that each calix[4]arene has two firm absorption peaks but different range transitions due to their molecular structures. FESEM images of N-DHC4 has shown the formation of almost spherical particles of calix[4]arene, while EDX analyses confirmed the elemental composition of the structural molecular of N-DHC4. Further observation has been done on the ΔV_{max} and μ_{max} of the two functionalized dihydroxycalix[4]arene for Pb^{2+} cation entrapments. By comparison, C-DHC4 has shown significant and stable results in detecting Pb^{2+} cations compared to N-DHC4. This work proves that this calix[4]arene is beneficial for further metal cation sensing field research.

Acknowledgements

This study has been carried out under Fundamental Research Grants Scheme 2020-0256-103-02 (FRGS/1/2020/STG07/UPSI/02/2) provided by the Ministry of Education of Malaysia. The authors would like to express their gratitude to Universiti Pendidikan Sultan Idris (UPSI), who helped manage the grants.

Author Contributions

All authors contributed toward data analysis, drafting and critically revising the paper and agree to be accountable for all aspects of the work.

Disclosure of Conflict of Interest

The authors have no disclosures to declare.

Compliance with Ethical Standards

The work is compliant with ethical standards.

References

[1] Azahari, N. A., Supian, F. L., Richardson, T. H. & Malik, S. A. (2014). Properties of Calix4 Lead(Pb) Films using Langmuir-Blodgett(LB) Technique as an Application of Ion Sensor. *Advanced Materials Research,* 895, 8-11.

[2] Razali, A. S., Supian, F. L., Salleh, M. M. & Bakar, S. A. (2015). Characterization and Detection of Cadmium Ion Using Modification Calixarene with Multiwalled Carbon Nanotube. *International Journal of Chemical and Molecular Engineering,* 9(2).

[1] Azahari, N. A., Supian, F. L., Richardson, T. H. & Malik, S. A. (2014). Properties of Calix4 Lead (Pb) Films using Langmuir-Blodgett(LB) Technique as an Application of Ion Sensor. *Advanced Materials Research,* 895, 8-11.

[2] Razali, A. S., Supian, F. L., Salleh, M. M. & Bakar, S. A. (2015). Characterization and Detection of Cadmium Ion Using Modification Calixarene with Multiwalled Carbon Nanotube. *International Journal of Chemical and Molecular Engineering,* 9(2).

[3] Lim C.K.D. & Supian, F. L. (2017). Elucidation Of Properties In Langmuir Monolayers And Langmuir - Blodgett (LB) Films Formed By Calix[6]arene. *Jurnal Fizik Malaysia,* 38(1) 010034 – 010043.

[4] Azmi, M. S. M., Noorizhab, M. F. F., Supian, F. L. & Malik, S. A. (2020). A Review of Calixarene Langmuir–Blodgett Thin Film Characteristics for Nanosensor Applications. *Defence S and T Technical Bulletin*, 13 205-216.

[5] de Silva, A. P., Gunaratne, H. Q. N., Gunnlaugsson, T., Huxley, A. J. M., McCoy, C. P., Rademacher, J. T. & Rice, T. E. (1997). Signalling recognition events with fluorescent sensors and switches. *Chemical Reviews*, 97 1515–1566

[6] Supian, F. L., Richardson, T. H., Deasy, M., Kelleher, F., Ward, J. P. & McKee, V. (2010). Interaction between Langmuir and Langmuir-Blodgett Films of Two Calix[4]arenes with Aqueous Copper and Lithium Ions. *Langmuir,* 26(13) 10906–10912.

[7] Lim, C. K. D., Supian, F. L. & Hamzah, Y. (2020). Langmuir, Raman, and Electrical Properties Comparison of Calixarene and Calixarene-rGO using Langmuir Blodgett (LB) Technique. *J Mater Sci: Mater Electron*, 31 18487–18494

[8] Patra, S., Maity, D., Gunupuru, R., Agnihotri, P. & Paul, P. (2012). Calixarenes: Versatile molecules as molecular sensors for ion recognition study. *Journal of Chemical Sciences,* 124 1287–1299.

[9] Shinkai, S., Mori, S., Koreishi, H., Tsubaki, T., & Manabe, O. (1986). Hexasulfonated calix[6]arene derivatives: a new class of catalysts, surfactants, and host molecules. *Journal of American Chemical Society,* 108 2409-2416.

[10] Asfari, Z., Bohmer, V., Harrowfield, J. & Vicens, J. (Eds.). (2001). *Calixarenes 2001*. Dordrecht: Springer Netherlands.

[11] Nostro, P. L., Capuzzi, G., Fratini, E., Dei, L. & Baglioni, P. (2001). Modulation of interfacial properties of functionalized calixarenes. *Progress in Colloid and Polymer Science*, 118 238-242.

[12] Yuan, Y., Zhang, B., Sun, J., Jonnard, P., Le Guen, K., Tu, Y., ... & Lan, R. (2020). Structure and optical properties of CrO x N y films with composition modulation. *Surface Engineering*, *36*(4), 411-417.

[13] Doménech-Carbó, M. T., Álvarez-Romero, C., Doménech-Carbó, A., Osete-Cortina, L., & Martínez-Bazán, M. L. (2019). Microchemical surface analysis of historic copper-based coins by the combined use of FIB-FESEM-EDX, OM, FTIR spectroscopy and solid-state electrochemical techniques. *Microchemical Journal*, *148*, 573-581.

[14] Jurak, M., Szafran, K., Cea, P., & Martín, S. (2021). Analysis of Molecular Interactions between Components in Phospholipid-Immunosuppressant-Antioxidant Mixed Langmuir Films. Langmuir, 37(18), 5601-5616.

[15] Chachaj-Brekiesz, A., Kobierski, J., Wnętrzak, A., & Dynarowicz-Latka, P. (2021). Electrical Properties of Membrane Phospholipids in Langmuir Monolayers. *Membranes*, *11*(1), 53.

[16] Liekkinen, J., de Santos Moreno, B., Paananen, R. O., Vattulainen, I., Monticelli, L., de la Serna, J. B., & Javanainen, M. (2020). Understanding the Functional Properties of Lipid Heterogeneity in Pulmonary Surfactant Monolayers at the Atomistic Level. *Frontiers in cell and developmental biology*, *8*.

[17] Supian, F. L., Richardson, T. H., Deasy, M., Kelleher, F., Ward, J. P. & Mckee, V. (2010). A Surface Potential Study of Ion-Uptake by 5,11,17,23-Tetra-Tert-Butyl-25,27 Diethoxycarbonyl Methyleneoxy-26,28,Dihydroxycalix[4]Arene and 5,17-(Nitrobenzylideneamino)-11,23-Di-Tert-Butyl-25,27- Diethoxycarbonyl Methyleneoxy-26,28-Dihydroxycalix[4]Arene Langmuir Blodgett (LB) Monolayers. *Sains Malaysiana*, 39(3) 423-433.

[18] Nostro, P. L., Casnati, A., Bossoletti, L., Dei, L., Baglioni, P. (1996). Colloids and surfaces A: physicochem. and engineering aspect, 116, 203.